



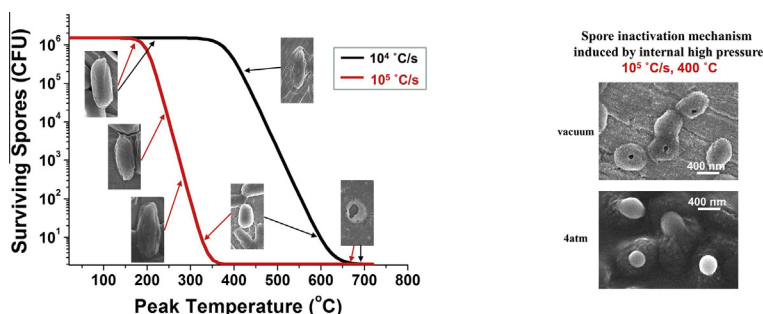
Inactivation of bacterial spores subjected to sub-second thermal stress

W. Zhou^a, M.W. Orr^c, G. Jian^b, S.K. Watt^c, V.T. Lee^{c,*}, M.R. Zachariah^{a,b,*}^a Department of Chemical and Biomolecular Engineering, University of Maryland, College Park, MD 20742, USA^b Department of Chemistry and Biochemistry, University of Maryland, College Park, MD 20742, USA^c Department of Cell Biology & Molecular Genetics, University of Maryland, College Park, MD 20742, USA

HIGHLIGHTS

- A new approach to quantitatively apply high rate heat stress is developed.
- Spore inactivation with temperature followed a sigmoidal behavior with higher heating rates improving the neutralization efficiency.
- The peak temperature and not heating time was responsible for spore inactivation at $\sim 10^4$ °C/s.
- Viability reduction was mainly due to DNA damage at $\sim 10^4$ °C/s.
- Spore inactivation was mainly due to internal pressurization at $\sim 10^5$ °C/s.

GRAPHICAL ABSTRACT



ARTICLE INFO

Article history:

Received 12 February 2015

Received in revised form 28 April 2015

Accepted 5 May 2015

Available online 14 May 2015

Keywords:

Bacterial spores

Inactivation

Ultrafast heating

Killing mechanism

ABSTRACT

Rapid heat pulse is the primary method for neutralizing large quantities of spores. Characterizing heat inactivation on a millisecond time scale has been limited by the ability to apply ultrafast, uniform heating to spores. Using our system for immobilization of spores on metal surfaces, bacterial spores were subjected to high temperatures (200–800 °C) and heating rates ($\sim 10^3$ °C/s to $\sim 10^5$ °C/s). Spore inactivation increased with temperature and fit a sigmoid response. We observed the critical peak temperature (T_c) which caused a 2-fold reduction in spore viability was 382 °C and 199 °C for heating rates of $\sim 10^4$ °C/s and $\sim 10^5$ °C/s, respectively. Repetitive heating to the same peak temperature had little effect on viability. In contrast, stepwise heating to elevated peak temperatures inactivated spores in a manner similar to a single pulse heating to the same peak temperature. These results indicate that the maximum temperature rather than the overall heating time is primarily responsible for spore neutralization at $\sim 10^4$ °C/s heating rate. The mechanism of spore inactivation was further investigated at two heating rates ($\sim 10^4$ °C/s and $\sim 10^5$ °C/s). Viability reduction was mainly due to DNA damage at the heating rate of $\sim 10^4$ °C/s as mutant strains defective for *sspA*, *sspB* and *recA* were more sensitive to heat than the wide-type strains. At the higher heating rate ($\sim 10^5$ °C/s), spore inactivation was correlated with physical damage from ultrafast vapor pressurization inside spores. This new approach of pulse heating generates a temperature, time, and kill relationship for *Bacillus* spores at sub-second timescales.

© 2015 Published by Elsevier B.V.

* Corresponding authors.

E-mail addresses: vtlee@umd.edu (V.T. Lee), mrz@umd.edu (M.R. Zachariah).

1. Introduction

Bacterial spores are a dormant cell type that are highly resistant to heat, moisture, pressurization, radiation and biocidal stresses [1–3]. Concerns regarding bio-terrorism [4] and possibly other public health risks [5,6] require the urgent development of methods for large scale inactivation of bacterial spores. The use of thermal destruction is a straightforward and convenient approach that has been investigated for the inactivation of spores in the liquid phase [7–16]. Conventional thermal inactivation methods require time periods up to minutes or even hours and are limited by a maximum temperature of 150 °C [8–10,11,13]. Maintaining these temperatures for the required time periods is unfeasible for large quantities of spores. Thus, stand-off neutralization methods which can sustain higher temperatures (>200 °C) for short periods of time (sub-seconds) are being considered, and these new temperature–time–kill histories of spore inactivation require evaluation. Aerosol methods have recently been employed to evaluate thermal and chemical kills of spores at extreme heating conditions [17–25]. These approaches have the advantage of isotropic and rapid heat transfer to individual spores, as well as controllable shorter heating times (milliseconds to seconds) and higher heating temperatures (>200 °C) [17–25]. However, there existed a temperature distribution within a population of spores in these studies, which allows for calculating the average resident time and temperature of the entire spore population, but not for individual spores. These studies evaluated the effect of peak temperature on spore viability. However, the effects of heating and cooling rates on spore inactivation were not discussed.

Precise measurements of heating rate and heating history can be achieved by an alternative method that heats spores immobilized on metal supports. Previous studies have shown that organic or inorganic nano/microparticles deposited on metal surfaces could be heated to a wide range of surface temperature (from ~100 °C to ~1800 °C) at a rate as high as ~10⁶ °C/s [26–31]. In those studies, the heating time could be controlled with millisecond precision and the heating rate could be accurately tuned from ~10³ °C/s to ~10⁶ °C/s, allowing the application of uniform temperature to a deposited particle layer up to 5 μm thick [29] which exceeds the dimensions of a monolayer of bacterial spores. This approach allows accurate application of a uniform high temperature over millisecond time scales for individual spores, which will aid in determining the temperature–time–kill relationship of spores at high temperatures and sub-second timescales.

The mechanism of spore inactivation has been primarily studied in conventional heating schemes. Major mechanisms of spore inactivation occurred through damage to DNA and proteins [3]. Evidence supporting killing by DNA damage includes several studies that found mutants depleted in the *sspA sspB* genes (coding for α/β-type small, acid-soluble proteins (SASP)) and *recA* genes (coding for RecA) were sensitized to mutagenesis and inactivation under dry heating schemes [32–36]. In the dormant spores, SASP bind genomic DNA [32,33] to prevent depurination and strand breakage thereby confer resistance to dry heat and ultraviolet irradiation [34,35]. RecA participates in recombination repair to remove DNA lesions caused by dry heat [36]. In contrast, denaturation of some key proteins such as metabolic enzymes was found as the mechanism of spore killing in wet heat [8,37]. However, the specific proteins to which denaturation induces spore inactivation have not been identified [38]. A second mechanism of inactivation is through permeabilization of the spore membrane, cortex and coat (encoded by genes like *cotE*), as supported by several lines of evidence [3,39–44]. Damage to spore compartments after heating has been shown with compartment-specific staining techniques [45,46]. While the spore coat was identified as the

primary barrier to oxidizing agents (hydrogen peroxide, hypochlorite, ozone, etc.) [47–49], the spore cortex plays a major role in maintaining spore resistance to heat [3,39]. Failure of the cortex structure leads to spore inactivation by two mechanisms. The first is the release of dipicolinic acid (DPA) associated with DNA damage during dry heating [40,41] and protein denaturation during wet heating [38]. The second is through rehydration of the spore protoplast [39,42]. Rehydration of the core will induce a concomitant reduction in spore heat resistance by disrupting SASP–DNA interaction and permitting protein denaturation [43,44]. Through these studies, the temperature–time–kill relationships for spores from several species have been characterized under conventional heating schemes [8–11,13]. However, the exact mechanism of spore inactivation during rapid heating, which is closer to conditions seen under combustion, is poorly understood. Recent studies of bacterial spores heated in hot air show that high-temperature gas induced severe damage to the spore core [50], and the extent of inactivation was attributed to the DNA damage [22].

In this work, we present the effect of fast heating pulses (~10⁴ °C/s and ~10⁵ °C/s) on surface-immobilized spores as a complementary approach to the aerosol studies. Our heating scheme possesses the advantages of precise measurement of heating time and rates, as well as uniform temporal temperature for individual spores. Using this heating scheme, we determined the effect of peak heating temperature and heat rate by assessing spore viability and morphology. The heating histories of spores were also investigated through repetitive exposures as a possible factor influencing spore inactivation. To investigate the mechanism of killing, spores carrying *sspA sspB*, *recA* or *cotE* mutations were tested to determine whether known mechanisms of spore inactivation contribute to spore viability in our heating scheme. Using these results, we propose a model for the thermal destruction of bacterial spores in the heating rates of ~10⁴ °C/s and ~10⁵ °C/s.

2. Materials and methods

2.1. Spore attachment on platinum wires

Bacillus subtilis (Bs) (ATCC#6051) were sporulated in Difco Sporulation Medium (DSM) at 30 °C for 48 h. The 250 ml of DSM included 2 g Bacto nutrient broth, 2.5 ml 10% KCl, 0.375 ml 1 M NaOH and 2.5 ml 1.2% MgSO₄·7H₂O. The spore concentration was enumerated by plating to be 8 × 10⁹ colony-forming units per milliliter (CFU/ml). The purity of spores was found more than 99%. For analysis of mechanism of killing, four isogenic Bs spore strains, namely, a wild-type strain (PS533) [36], a Δ *cotE* mutant strain lacking coat (PS3328) [48], a Δ *sspA* Δ *sspB* mutant strain lacking DNA protection mechanism (PS578) [32], and a Δ *recA* mutant strain lacking DNA repair mechanism (PS2318b) [36] were generously provided by Dr. Peter Setlow (University of Connecticut). A platinum (Pt) wire with a diameter of 76.8 μm (Omega Engineering, Inc.) was used to immobilize spores. An in-house spore deposition cell was manufactured for coating the wire with Bs spores electrophoretically (Fig. S1). By controlling the biased deposition voltage, pulse frequency, and charging time (from a 6340 sub-femtoamp remote source, Keithley), a uniform monolayer of spores in the central region of the wire (~1 cm) could be obtained (Fig. 1A). The detailed information of the spore deposition cell and charging conditions can be found in our previous work [51].

2.2. Wire heating test

To subject spores to a defined thermal history, the spore coated Pt wire was connected to an in-house built power source, working

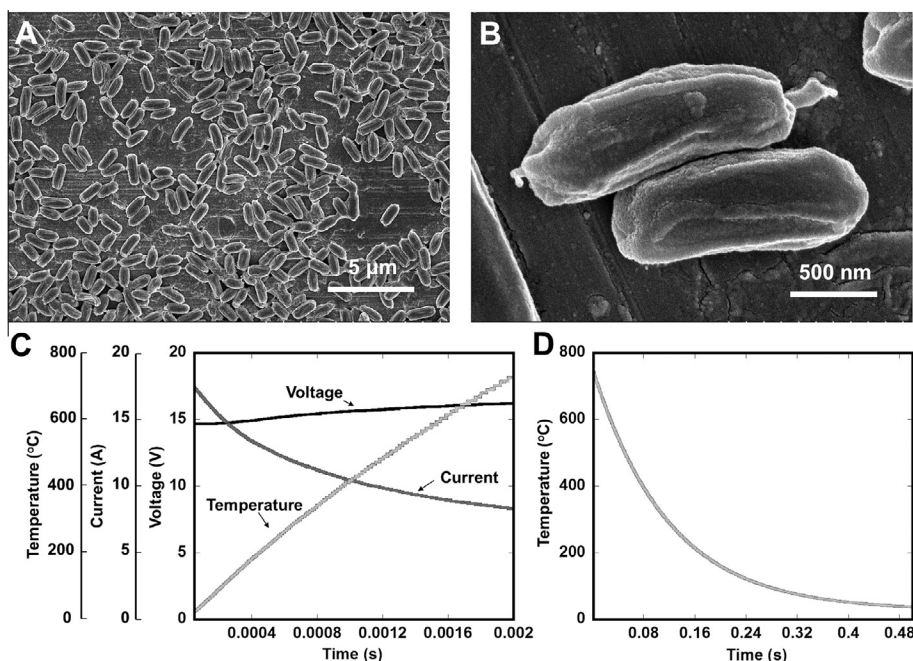


Fig. 1. (A) Electrophoretically deposited monolayer of Bs spores on the Pt wire as imaged by SEM. (B) High magnification SEM image of two immobilized spores. (C) Example of voltage, current and temperature temporal traces on the Pt wire surface in a 2 ms pulse test. The maximal temperature is ~ 740 °C in this case. (D) Surface temperature of the wire after cessation of the heating pulse.

as a temperature jump probe (Fig. S2). A pulse signal was generated to trigger the power supply prior to the heating of wire in air. The applied voltage (supplied from a 6291A DC power supply, HP) and the measured current (by a current probe AM503, Tektronix) were simultaneously recorded via an oscilloscope (LT344, LeCroy). The transient temperature on the wire during the heating period was measured based on the standard dynamic electric resistance temperature relationship (Callendar–Van Dusen equation) [52], in which the resistance measured from the applied voltage and the current was in a quadratic relationship with the transient temperature (see details in Supplemental text, Eqs. (S1)–(S9)). The maximum temperature (~ 200 °C to ~ 800 °C) and the heating rate ($\sim 10^3$ °C/s to $\sim 10^5$ °C/s) can be precisely controlled by varying the applied voltage and the pulse time (2–50 ms). The corresponding profile of the wire in the cooled region was calculated according to an energy balance equation which was dominated by the heat conduction. The detailed content of the mathematical modeling can be found in the Supplemental information. The spore-coated Pt wire was replaced after each heating test, and the heated wires were processed for SEM imaging and determination of CFUs.

For wire heating tests in different pressures, two home-built chambers were used. The first chamber was connected to a vacuum pump for spore heating experiments under pressures as low as $\sim 10^{-5}$ Pa, while the second chamber was connected to a high-pressure air source for experiments under pressures up to 4×10^5 Pa.

2.3. Determination of colony forming units

The number of viable spores that survived various heating conditions was enumerated by determining CFUs. Wires coated with heated or unheated spores were completely submerged in 1 ml of Lysogeny Broth (LB) media (10 g tryptone, 5 g yeast extract and 5 g NaCl per liter) and placed on a shaker at the 37 °C for three hours to allow for the germination and detachment of viable spores from the wire surface. After incubation, samples were serially

diluted and plated on LB agar plates to determine viable CFUs. Each test included at least six replicates. The relationship of the recovered counts with time is shown in Fig. S3. Previous SEM images of unheated wires showed that $\sim 10^6$ spores were coated onto the platinum wires [51]. The three hours incubation time resulted in CFU counts that reflect the 10^6 spores on the wire.

The validity of this spore counting protocol was also evaluated by *in situ* phase contrast microscopy (Zeiss LSM 710, Germany) to monitor the germination of spores from wires. We found that Bs spores took 1 h before transition from phase bright to phase dark, and the 2 h to completely detach from wires. Additional experiments were performed on wire heated to temperatures >600 °C, a temperature that sterilizes Bs spores (see Fig. 2). Prolonged incubation of these heated wires for 24 h in LB at 37 °C failed to yield any growth.

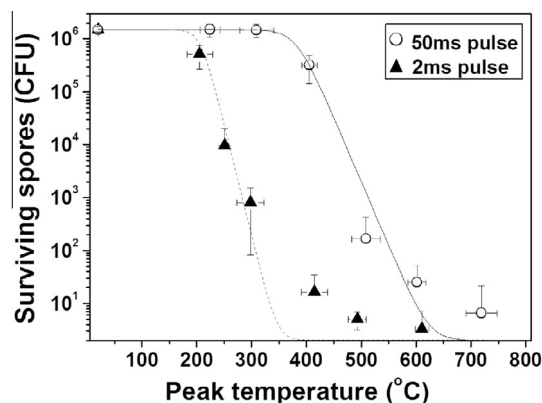


Fig. 2. Survival curves of Bs spores versus peak temperature for 2 ms and 50 ms heat pulses. Each experimental point represents the average of at least 6 replicates, and the standard deviations both in the measured spore viabilities and peak temperatures are indicated.

2.4. Spore morphological characterization

The heated wires were first mounted to stubs and then sputtered with gold/palladium alloy prior to the SEM using Hitachi S-4700). The dimensions of the spores were assessed by two parameters measured from SEM images, namely the aspect ratio (length divided by width) and the projected area (surface area inside the contour line of the cell body) of spores on the Pt surface. Statistical analyses are based on a spore population of >50.

2.5. Estimation of vapor pressurization inside spores

The vapor pressure and temperature relationship was calculated by a simple closed model assuming the spore allows for heat but not mass transfer. Empirical thermodynamics data of superheated vapor and steam were used to plot the standard curve of pressure rise with temperature (see details in the [Supplemental information](#)).

3. Results

3.1. Temperature profiles of the Pt wire surface

Precise definition of the temperature–time–kill relationship for Bs spores in sub-second time scales requires accurate and fast measurement of the spore temperature. Joule heating triggered by a strong electrical pulse enables us to quickly and accurately measure the transient temperature in a sub-second heating process. Our temperature–time measurement shows that the transient temperature on the wire surface during heating followed a closely linear ascending trace ([Fig. 1C](#)), while temperature–time calculation based on radial heat transfer estimates a slow exponential decaying trace when the pulse was turned off ([Fig. 1D](#)). The temperature of the ascending trace was measured from the time dependent variations of the applied voltage and current (see [Eq. \(S3\) in the Supplemental information](#)). By tuning the pulse time (2–50 ms) and applied voltage, different maximum temperatures (200–800 °C) and heating rates ($\sim 10^3$ °C/s to $\sim 10^5$ °C/s) could be obtained ([Fig. S5](#)). The temperature decaying trace was calculated from a radial heat transfer model by assuming that most heat loss occurred by conduction from the cylindrical wire surface (see

details in [Supplemental text, Eqs. \(S1\)–\(S9\)](#)). The surface temperature dropped exponentially after the voltage was turned off and returned to 40 °C after ~ 300 ms to ~ 500 ms ([Table S1](#)). While these cooling times are longer than the heating pulse times (2–50 ms), they are much shorter than the times employed in previous protocols [[12,14](#)].

3.2. Spore viability heated to fixed peak temperatures at two ramp rates

We assessed the effect of fast heating on the viability of Bs spores. When exposed to 50 ms fast heating pulse, spores reached peak temperatures between 200 °C to 800 °C which represents heat rates of 4×10^3 to 2×10^4 °C/s. Peak temperatures below 350 °C had minimal effect in the spore viability ([Fig. 2](#)). Once the temperature reached over 350 °C, the viability of spores decreased sharply by ~ 5 logs from 350 °C to 600 °C. Further increases in the peak temperature to ~ 700 °C reduced spore viability by 6 logs. These results indicate that 400 °C was the maximum peak temperature that the spores could resist in the 50 ms heating scheme.

When exposed to a 2 ms ultrafast heating pulse, spores reached peak temperatures between 200 °C to 800 °C, however, the heat rates were higher (1×10^5 to 4×10^5 °C/s). The spores were inactivated at a lower peak temperature (180 °C) and a reduction of 5 logs was achieved at 400 °C compared with 600 °C in 50 ms pulse heating. Finally, a complete viability reduction of 6 logs was reached at temperatures over 500 °C. These results indicate the time–temperature–kill relationships at different heating rates show similar sigmoidal response. However, the faster heating rate of $\sim 10^5$ °C/s potentiates spore inactivation and effectively reduces the peak temperature required for 6-log spore neutralization when compared to the heating rate of $\sim 10^4$ °C/s.

The viability data above were fitted with a standard sigmoid model used in traditional low rate heating experiments [[53](#)] as follows:

$$S = \frac{1}{1 + \exp(k(T - T_c))} \quad (1)$$

where S is the survival ratio of spores ($CFU_{\text{final}}/CFU_{\text{initial}}$), T is the peak temperature in a heating event, T_c is the critical peak temperature at which the spore viability is reduced by half, and k is the heat resistance parameter (larger k means spore viability is more temperature sensitive). In our study, the initial number of spores on the wire was measured as $\sim 1.5 \times 10^6$ CFU. The fitted values of T_c and k are listed in [Table 1](#). We found that the k value of the curve representing the spore destruction at the higher heating rates ($\sim 10^5$ °C/s) was larger than that of the lower heating rates ($\sim 10^4$ °C/s) ([Table 2](#)). In addition, T_c at the heating rates of

Table 1
Fitting results for the variables in Eq. (1).

Heating conditions	k (°C ⁻¹)	T_c (°C)
2 ms heating pulse ($\sim 10^5$ °C/s)	0.096	199
50 ms heating pulse ($\sim 10^4$ °C/s)	0.056	382

Table 2
Changes to spore physical dimensions after 2 ms and 50 ms pulse heating to different temperatures, with related viability loss.

Heating conditions	Length (μm) ^a	Width (μm) ^a	Aspect ratio	Projected area (μm^2) ^b	Viability (CFU)
Unheated	1.54 ± 0.17	0.62 ± 0.05	2.49 ± 0.37	0.82 ± 0.09	1.5×10^6
2 ms pulse, heat to 200 °C	1.47 ± 0.17	0.62 ± 0.02	2.38 ± 0.28	0.82 ± 0.10	7.8×10^5
2 ms pulse, heat to 240 °C	1.40 ± 0.14	0.61 ± 0.03	2.32 ± 0.31	0.82 ± 0.07	1.7×10^4
2 ms pulse, heat to 300 °C	1.49 ± 0.14	0.60 ± 0.04	2.43 ± 0.25	0.84 ± 0.11	5.7×10^1
2 ms pulse, heat to 410 °C	1.11 ± 0.11	0.56 ± 0.05	1.98 ± 0.21	0.52 ± 0.05	2.0×10^1
2 ms pulse, heat to 520 °C	0.69 ± 0.05	0.60 ± 0.07	1.16 ± 0.15	0.36 ± 0.04	0
50 ms pulse, heat to 170 °C	1.45 ± 0.13	0.59 ± 0.03	2.46 ± 0.29	0.79 ± 0.09	1.5×10^6
50 ms pulse, heat to 410 °C	1.11 ± 0.09	0.44 ± 0.04	2.57 ± 0.30	0.43 ± 0.02	2.4×10^5
50 ms pulse, heat to 570 °C	0.81 ± 0.10	0.54 ± 0.05	1.56 ± 0.21	0.44 ± 0.04	4.2×10^1

Data are derived from a random sample of 15 spores from totally more than 50 spores in SEM images.

^a The length and width were measured as the longest distances along the longitudinal and transverse directions of the spore body.

^b The projected area does not represent the spore volume, but acts as a comparable variable to evaluate changes in dimension under different heating conditions.

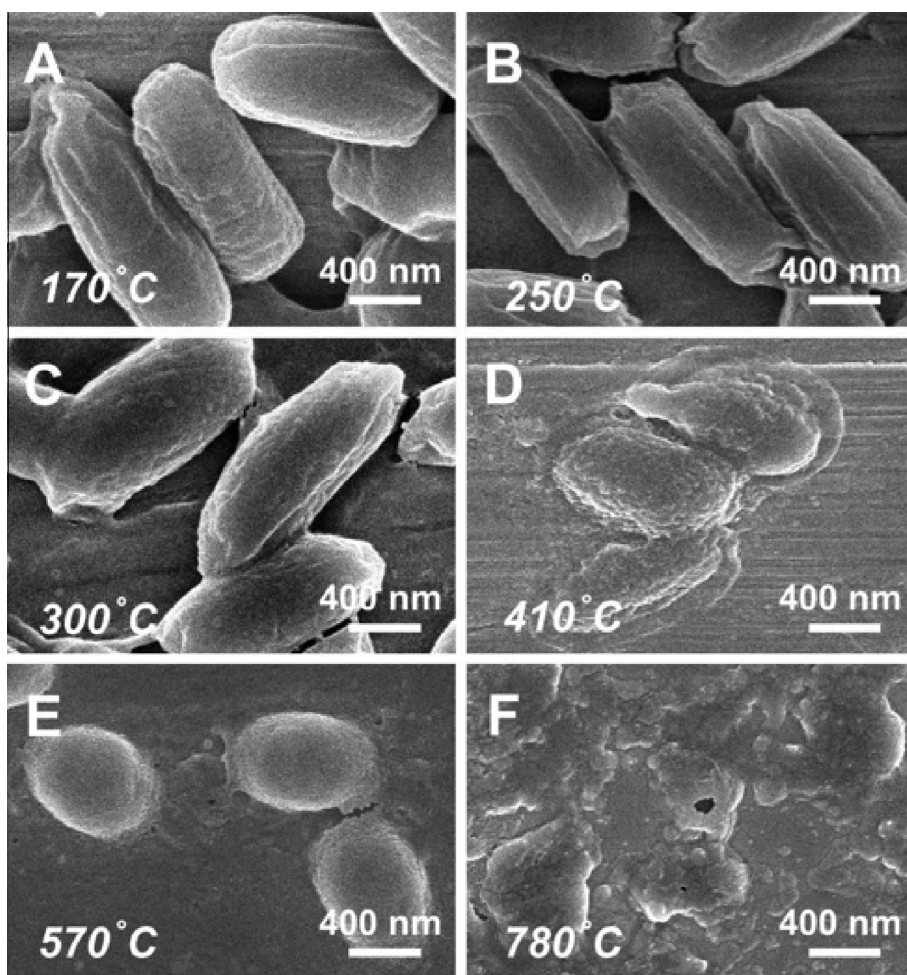


Fig. 3. SEM images of surface attached Bs spores after heat treatment triggered by a 50 ms pulse ($\sim 10^4$ °C/s). Each image shows a representative morphological change of over 50 spores (see Fig. S6). The maximum temperatures exerted on spores are indicated (A–F).

$\sim 10^5$ °C/s was lower than that at the heating rates of $\sim 10^4$ °C/s. Together, these results indicate that ultrafast heating rates ($\sim 10^5$ °C/s) potentiate spore inactivation.

3.3. Spore morphology after heating to defined peak temperatures at two ramp rates

We assessed the morphological features of spores after heating. The unheated spores had characteristic longitudinal ridges along their surfaces (Fig. 1B). At the heating rates of $\sim 10^4$ °C/s, after fast heating to a peak temperature of up to 300 °C, the aspect ratio and the projected area remained constant (Fig. 3A and Table 2). Fast heating to 410 °C caused spores to shrink (projected area on surface decreased by 48% to $0.43 \mu\text{m}^2$) (Fig. 3B). When heated to 570 °C (Fig. 3C), the spores were rounded (aspect ratio decreased by 37% to 1.56) without additional reduction in spore size (projected area decreased by 46% to $0.44 \mu\text{m}^2$). The spore surface lost its integrity after fast heating to 780 °C (Fig. 3D). These results indicate that the severity of morphological change under the fast-heating and high temperature conditions correlates with spore viability at the heating rates of $\sim 10^4$ °C/s (Figs. 2 and 3 and relevant low magnification Fig. S6).

We also investigated the morphology of spores exposed to faster heating (2 ms pulses, $\sim 10^4$ °C/s). When heated to temperatures below 300 °C, the aspect ratio and surface area remained unchanged even though there was a large reduction in spore

viability (Figs. 2 and 4B). At peak temperatures of 300 °C and above, pin holes and fissures were observed (Figs. 4C, S7 and S8). When heated to 410 °C, the aspect ratio decreased by 21% to 1.98 and the projected area decreased by 38% to $0.52 \mu\text{m}^2$ (Fig. 4D). At a peak temperature of 520 °C, the aspect ratio further decreased by 53% to 1.16 and the projected area reduced by 56% to $0.36 \mu\text{m}^2$ (Fig. 4E). By comparing spores exposed to the same peak temperature at two different heating rates, spores exposed to the faster heating rate ($\sim 10^5$ °C/s) have minor morphological changes despite increased inactivation (Table 2, Figs. 3 and 4). These results indicate that the spore killing mechanisms in two heating rates are different.

3.4. Effect of repetitive fast heat pulses ($\sim 10^4$ °C/s) on the spore morphology and viability

Our observations that faster heating rates and higher peak temperatures caused greater spore damage led us to propose a hypothesis that these two parameters have distinct effects on spores. To test this hypothesis, we devised two experiments to distinguish the effects of heating rate versus those of peak temperature. In the first experiment, we asked if repeated application of the same fast heating scheme resulted in accumulated damage to the spore (Fig. S9). The viability results show that spores exposed to 20 rounds of 200 °C in 50 ms decreased the survival rate by less than one order of magnitude, demonstrating that the viability loss in the

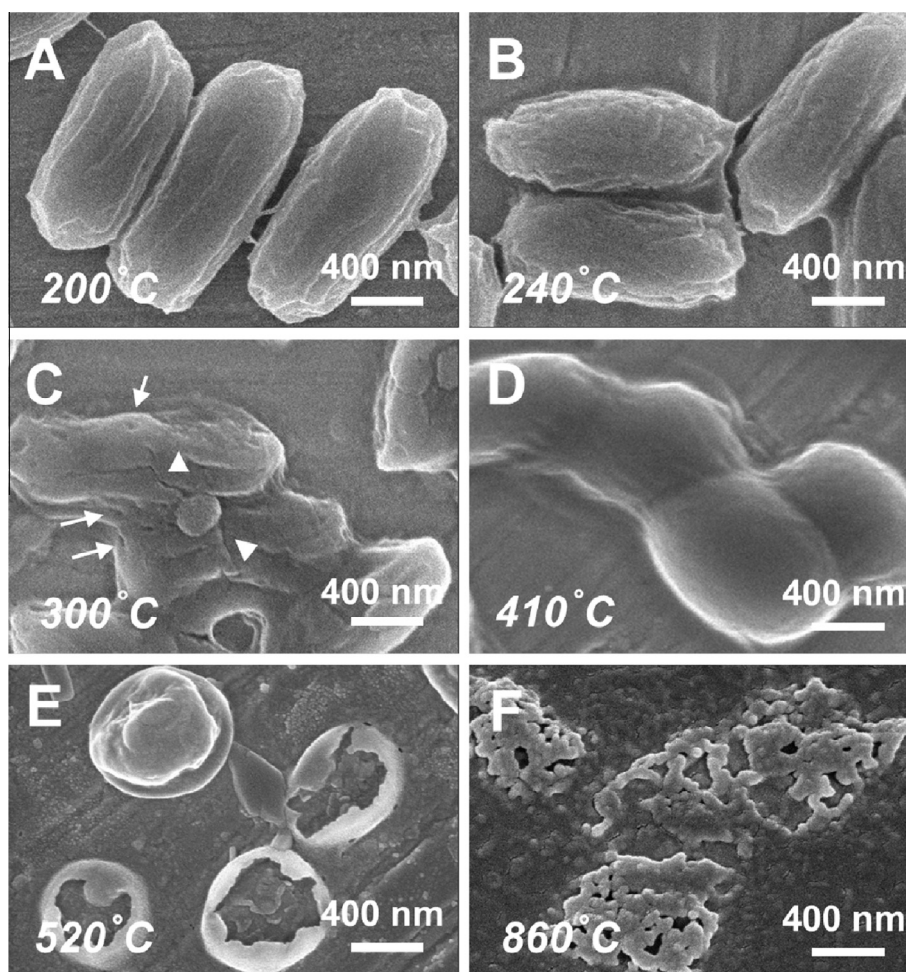


Fig. 4. SEM images of surface attached spores after heat treatment triggered by a 2 ms pulse ($\sim 10^5$ °C/s). Each image shows a representative morphological change of over 50 spores (see Fig. S7). The maximum temperatures exerted on spores are indicated (A–F). In (C), the arrows and the arrow heads indicate the location of holes and fissures on the spore surfaces, respectively.

first pulse is not additive (Fig. 5). SEM results also confirmed that spores exposed to different heating cycles of 400 °C in 50 ms showed minor morphological differences or size changes (Figs. 5 and S10 and Table S3). In the second experiment, we asked if the repeated exposure of treated spores to higher peak temperatures caused additional damage to spores (Fig. S11). Pre-heating to 200 °C in 50 ms prior to pulse heating to 500 °C in 50 ms did not alter the viability of spores compared to just heating to 500 °C in 50 ms (Fig. 5A). The resulting SEM images (Fig. 5B–F) also show that melted and disintegrated spore structures appeared when the second and third pulse peak temperatures increased to 600 °C and 800 °C, respectively. These morphological changes could also be achieved by singular pulse heating to corresponding peak temperatures. Considering the total heating time in our experiments is less than 10 s, we propose that the heat accumulation is negligible compared with the reported heating time in traditional spore decontamination studies that was normally minutes or even hours [8–10,11,13]. These results demonstrate that maximum peak temperature, rather than repetitive heating, is the primary determinant for spore morphology and viability when exposed to fast heating rates ($\sim 10^4$ °C/s).

3.5. Mechanism of inactivation by fast pulse heating ($\sim 10^4$ °C/s) through analysis of mutant spores

To understand the mechanism of spore inactivation under our fast heating scheme ($\sim 10^4$ °C/s), we have utilized wild-type strain

PS533 [54] and three mutant spore strains: (1) Strain PS3328 lacks *cotE* gene [55] which encodes a protein required for outer coat assembly [56]; (2) Strain PS578 has deletions in *sspA sspB* genes [54] which encodes SASP that bind and protect DNA in spores [3,57]; Strain PS2318b lacks *recA* gene [36] which encodes a protein required for DNA repair. Wide-type spore strain (PS553) and PS3328 retained similar viability at 300 °C (Fig. 6). In contrast, PS2318b and PS578 mutants had significant viability reductions by 1–3 logs at peak temperatures around 300 °C (Fig. 6), indicating that the DNA-repair proteins and SASP protect the *Bs* spore against fast heating pulse. At peak temperatures >400 °C, wild-type and all the three mutant spores had similar viability reductions of ~ 4 logs (Fig. 6). Surface attached spores heated at $\sim 10^4$ °C/s under dry conditions had similar mechanism of killing as *Bs* spores heated in aerosols [22]. However at higher rates of $\sim 10^5$ °C/s, viabilities of most of mutant spores and wild-type spores were reduced similarly by ~ 4 logs at peak temperatures of as low as 300 °C, indicating that the spore killing mechanism at higher heating rates of $\sim 10^5$ °C/s is not only due to DNA damage (Fig. S12).

3.6. Heat inactivation of spores at $\sim 10^5$ °C/s under different external pressures

We hypothesized that ultrafast heating at rates $>10^5$ °C/s inactivate spores by increasing the internal pressure within the spore (see Section 4). We tested this hypothesis by heating spores exposed to different external pressures. When heated at rates

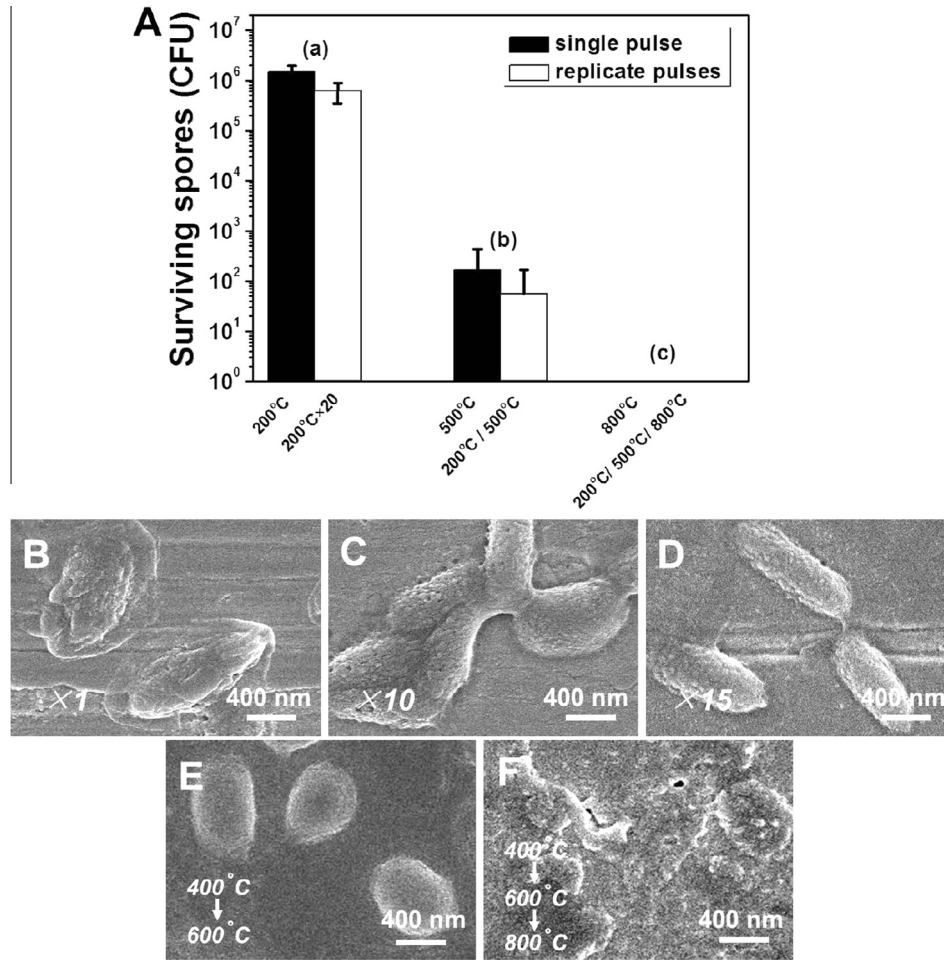


Fig. 5. Effect of repeat heat treatment on spore viability. (A–a) CFU of spores after being heated to 200 °C once (black bar) or 20 times (white bar) in the 50 ms pulse heating test. (A–b) CFU of spores after being heated to 200 °C followed by 500 °C (white bar), or directly heated to 200 °C (black bar) in the 50 ms pulse heating test. (A–c) CFU of spores after being heated in triplicates to 200 °C, 500 °C, and 800 °C subsequently (white bar), or directly heated to 800 °C (black bar) in the 50 ms pulse heating test. Bars are not shown in (A–c) since CFU = 0. Results are an average of at least 6 replicates and standard deviation is shown. In SEM images of (B)–(D), the heating pulse of 50 ms was tuned to yield the maximum temperature of ~400 °C. Samples were heated in (B), (C) and (D) for 1, 10 and 15 times, respectively. In (E), spores were first heated to 400 °C followed by a second pulse which heated spores to 600 °C. In (F), spores were heated to 400 °C, 600 °C and 800 °C under serial 50 ms pulses.

$>10^5$ °C/s in vacuum (1.3×10^{-5} Pa) with a peak temperature of 400 °C, holes formed on the spore surface indicating possible release of volatile species inside spores (Fig. 7). When spores were fast heated under 4 atm pressure (4.0×10^5 Pa) to 400 °C, bulges were observed on the surface of the spores indicating that volatile release was contained by the higher external pressure (Fig. 7). These results support our hypothesis that pressurization at heating rates of $\sim 10^5$ °C/s was associated with volatile release, thus contributing to spore inactivation.

4. Discussion

4.1. Temperature profiles of *Bs* spores on the Pt wire surface

Do *Bs* spores reach the same temperature as the Pt wire? Previous studies have revealed rapid heat transfer from the environment to the spore. Kumar et al. [58] showed that the spore took ~ 0.1 ms to reach the surrounding temperature of ~ 400 °C. Xing et al. [59] showed that the temperature could reach steady state in less than 0.5 ms. Since our spores are directly in contact with

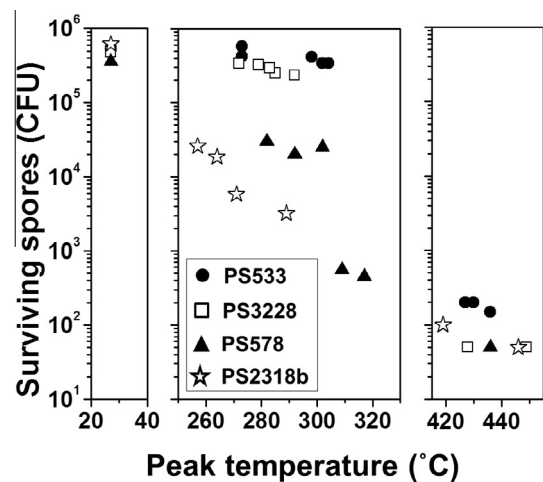


Fig. 6. Survival counts of the wide-type strain (PS533) and three mutant strains (PS3328 ($\Delta cotE$), PS578 ($\Delta sspA \Delta sspB$) and PS2318b ($\Delta recA$)) of *Bs* spores at elevated peak temperatures in the 50 ms pulse heating.

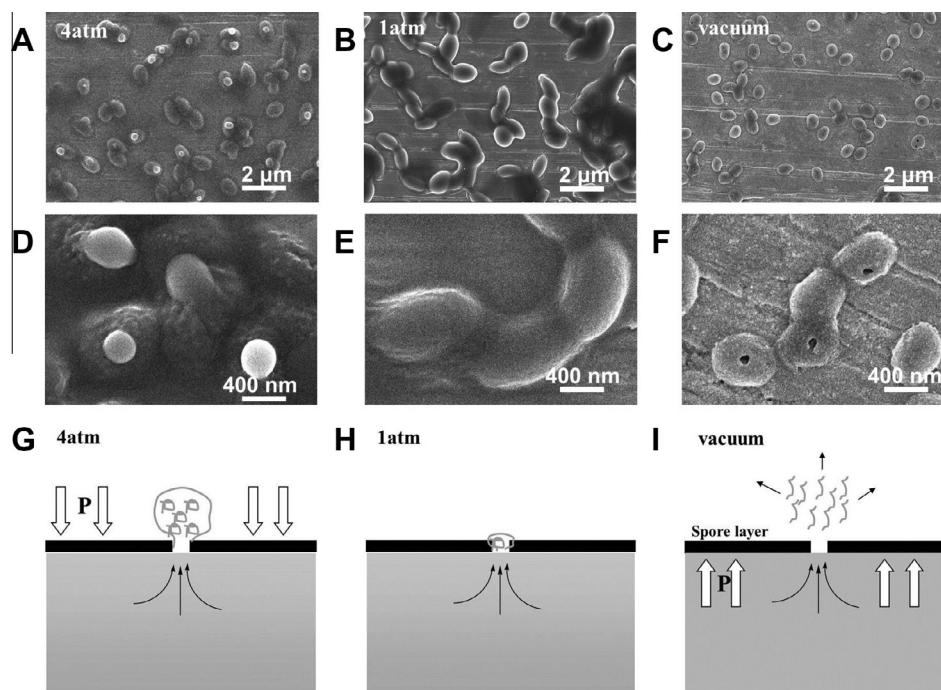


Fig. 7. Effect of external pressure towards the morphological changes of spores heated to 400 °C at a heating rate of $\sim 10^5$ °C/s. The pressures applied to spores in image (A), (B), and (C) are 4.0×10^5 Pa, 1.0×10^5 Pa, are 1.3×10^{-5} Pa, respectively. (D), (E), and (F) are the enlarged SEM images of (A), (B), and (C), respectively. (G), (H), and (I) are schematic drawings of the effect of external pressure towards distinct spore morphologies.

the wire (Fig. 1), the temperature increase of the spores will approximate the temperature increase of the wire in a 2–50 ms pulse heating process. We also assessed the accuracy of our temperature measurements and the distribution of heat along the length of the wire by using blackbody calibration, which showed that the wire temperature measurement fit to theoretical values precisely, especially below 1000 °C. Unlike the reported temperature measurements using thermocouples in the gas-phase spore inactivation studies that show a certain spatial temperature distribution [17–25], our results show a narrow temperature distribution along the entire length of the wire (see the evenly distributed temporal light intensity on wire in Fig. S4).

4.2. Spore viability heated to fixed peak temperatures under the same pulse time

There is intense interest in characterizing inactivation of *Bacillus* spores by sub-second heating pulses. Here we compare and contrast the results from thermal inactivation of spores affixed to solid surfaces to other studies. In general, sub-second heat inactivation of spores has a sigmoid temperature–kill relationship. Gates et al. [18] implemented pressure shocks to rapidly increase the air temperature around aerosolized *Bs* spores to 200–700 °C within 2–45 ms. The loss of viability occurred at ~ 200 °C, followed by decrease by 5 logs from 200 °C to 500 °C. Further reduction in viability at higher temperatures was minimal. Grinshpun et al. [19,20] exposed aerosolized *Bs* spores to hot air flow (150–1000 °C) and controlled the entire exposure time to be around 0.2–1 s. Due to rapid heat transfer into aerosolized spores [58], the exact time to reach peak temperature could be much shorter. Similarly, the viability of spores started to decrease at 200–250 °C. From 250 °C to 370 °C, the viability dropped exponentially by 5 logs. Recently, Xing et al. [59] utilized a conductive heating system to rapidly heat *Bacillus anthracis* spores placed on a gold foil in 0.1 s. They found that the viability decreased exponentially with temperature, with a reduction of 5 logs from 300 °C to ~ 700 °C. All

these studies show clear correlations between temperature, heating time and spore inactivation efficiency. Although the temperature–kill curves from previous studies [18–20,59] are similar to our results (Fig. 2), the spore inactivation mechanisms are different. Grinshpun et al. [19,20] heated aerosolized dry spores through a top-hat heating scheme and found the primary contribution to spore inactivation was the peak temperature and the heating time. Gates et al. [18] killed spores in a gas dynamic heating scheme induced by mechanical shocks, in which the high pressure and top-hat temperature have synergistic effect on spore inactivation. However, the heating rate was not directly measured in these studies as an important factor. Our studies demonstrate that $\sim 10^5$ °C/s heating schemes can potentiate spore inactivation (Fig. 2).

The sigmoid nature of spore destruction kinetics is consistent with the kill curves within other time–kill models. Spores are resistant to applied heat during a short period of time, while suffered from rapid inactivation by 3–6 logs when the heating time is elongated [60]. Further increasing the heating time can induce complete inactivation of the few surviving spores [53]. Compared with these well-studied time–kill models, studies of temperature–kill relationships have been limited due to the narrow temperature range of conventional heating methods. Our temperature–kill results demonstrate a similar sigmoid feature for spore inactivation. There are also three stages relative to the T_c . At temperatures well below the T_c , spores are resistant to thermal damage. At temperatures near the T_c , the spores are readily inactivated and the survival ratio drops logarithmically. At temperature well above the T_c , the remaining spores are completely inactivated.

4.3. Relationship of spore morphology heated to defined peak temperatures at two ramp rates

We observed two different morphological changes at the two different heating rates. When heated at $\sim 10^4$ °C/s rate that is similar to other heating scheme studies, we find that increasing

severity of morphological change correlates with decrease in spore viability. Our results here demonstrate that when Bs spores heated to 400 °C at $\sim 10^4$ °C/s, a reduction of 38–42% in the projected area of spores was induced (Table 2). This reduction in projected area matches the ratio of areas of the spore cortex and the spore coat from previous observations made by TEM of spore thin sections [2,61,62]. From these TEMs, we calculated the projected areas of the intact spore with coat and the spore that has shed the coat, and estimated the reduction in the projected area to be between 32% and 40% based on the removal of the coat (Table S2). In contrast when spores exposed to $\sim 10^5$ °C/s heating rate, the spore viability decreased rapidly at temperatures above 200 °C. However, the aspect ratio and projected area remain unchanged. The exact correlation between the mechanical changes of spores from morphological studies and the spore inactivation efficiency remains to be determined. These results suggest that spores exposed to these higher heating rates ($\sim 10^5$ °C/s) are inactivated by a different mechanism than spores inactivated at $\sim 10^4$ °C/s.

4.4. Spore inactivation at fast heating rates ($\sim 10^4$ °C/s) through DNA damage

We determined the mechanism of heat inactivation of spores affixed on surfaces by utilizing mutant strains defective for DNA protection, DNA repair and coat assembly. We used the fast heating rate ($\sim 10^4$ °C/s) that allows detection of increased sensitivity in mutant spores. Our results show that DNA damage is a major contributor to inactivation of surface attached dry spores in the fast heat scheme, which is consistent with the mechanism for inactivation of aerosolized spores exposed to extreme dry heat [22,50]. Spore coat is not required for heat resistance in this heating scheme which agrees with results by Setlow et al. [3,63] that demonstrated that decoated spores had similar heat resistance to the wide-type spores. Instead, they found that the spore coat was mainly involved in resistance to some biocidal chemicals [47–49]. In agreement with the *cotE* mutant analysis, our morphological studies also show that when heated at $\sim 10^4$ °C/s spores with melted coats at 400 °C had minimal reduction in viability (Fig. 3B). Together, our results indicate that surface attached spores heated in our fast heating scheme ($\sim 10^4$ °C/s) behave similar to dry spores heated in other aerosol heating schemes [17–25].

4.5. Spore inactivation at heating rates of $\sim 10^5$ °C through rapid pressurization inside spore

Our results yield an interesting finding: when heated to the same peak temperature, higher heating rates of $\sim 10^5$ °C/s potentiate thermal inactivation of spores as compared to $\sim 10^4$ °C/s (see the temperature range from 250 °C to 450 °C in Fig. 2). What is the basis for enhanced spore inactivation by these higher heating rates? Since the peak temperature in these two heating schemes is the same, the observed enhanced killing of Bs spores must be due to the rate of heating (Fig. 2). We propose that this effect is due to vaporization of the internal contents of the spore, i.e. water, DPA and other volatiles. SEM images of spores heated at the $\sim 10^4$ °C/s revealed that the spores had minimal morphological change until >400 °C (Fig. 3 and Table 2). In contrast, SEM images of spores heated at $\sim 10^5$ °C/s formed the cracks and fissures at temperatures as low as 300 °C (Figs. 4C and S8). Spore viability was reduced at a lower peak temperature of 240 °C (Fig. 2) without detectable morphological change (Fig. 4), suggesting that transient holes may form in the spore coat that is not detectable by SEM (Fig. 4B). We tested whether pressurization events are occurring on the heated spore by testing the effect of external pressure on spore morphology. Spores on a wire were heated to the same peak temperature at $\sim 10^5$ °C/s in three different pressures: (1) vacuum,

(2) atmospheric (1 atm), and (3) four atmosphere (4 atm) pressure. Under vacuum, the spores displayed an exaggerated morphology in which large holes were formed (Fig. 7C and F). In contrast, SEMs of spores heated in excess external pressure showed ‘balloons’ on the surface of spores indicating that the external pressure contained the expansion of explosive volatiles (Fig. 7A and D).

Based on these observations, one possible mechanism for enhanced killing at ultrafast heating rates is the *dynamic* internal pressure generated by violent vaporization of volatiles, including water that imposes dynamic shock on spores. To estimate the *dynamic* internal pressure within spores during these heating events, we assumed that water is the primary volatile component in the cell since water comprises $\sim 30\%$ of the spore core mass [64]. Assuming minimal diffusive loss, and all liquid water is vigorously vaporized after 200 °C due to the rapid heating rates, *dynamic* pressure is a function of peak temperature [65]. Using the amount of water presented in the spore core and the volume of the spore core, the *dynamic* pressures at 240 °C and 400 °C are estimated to be 308 MPa and 404 MPa, respectively (Fig. S13). Based on our killing curves (Fig. 2) and morphological changes (Figs. 3 and 4), the maximum *dynamic* internal pressures that spores can sustain (without significant reduction of viability and failure of spore coat) are 308 MPa at a heating rate of $\sim 10^5$ °C/s, and 404 MPa at a heating rate of $\sim 10^4$ °C/s. This huge difference in the yield stresses indicates that the assumption of minimal diffusive loss of volatiles from the spore core must be incorrect. If we assume the diffusive rate of water through the spore coat keeps constant at ν (MPa/ms) during the temperature range of 240–400 °C, the real yield stress of spore coat (σ_{yield}) at both heating rates can be express as:

$$\sigma_{yield} = P_1 - \nu T_1 = P_2 - \nu T_2 \quad (2)$$

P_1 (308 MPa) and P_2 (404 MPa) are the maximum *dynamic* internal pressures of spores at heating rates of $\sim 10^5$ °C/s and $\sim 10^4$ °C/s, respectively. T_1 (2 ms) and T_2 (50 ms) are the pulse heating times at heating rates of $\sim 10^5$ °C/s and $\sim 10^4$ °C/s, respectively. The results are $\nu = 2$ MPa/ms and $\sigma_{yield} = 304$ MPa. Considering that the water diffusion rate (2 MPa/ms) is closer to the pressurization rate (8 MPa/ms) at $\sim 10^4$ °C/s, but much smaller than the pressurization rate (154 MPa/ms) at $\sim 10^5$ °C/s, it is easy to understand the potentiation of thermal inactivation at higher heating rates by internal pressurization. A similar explanation for spore inactivation was reported by Xing et al. [59]. They found that the spore surface was ruptured after rapid heating to 300 °C for 10 s, suggesting the vaporized content inside spores cannot promptly diffuse out and therefore the pressure-induced mechanical stresses exceed the yield stress of spores. The authors measured the temporal modulus of spores with temperature and found the modulus to be ~ 400 MPa at 275 °C [66]. We should also note that the maximum hydrostatic pressures (400–800 MPa) employed in the industrial high-pressure sterilization approaches [67–69] are larger than our aforementioned result (304 MPa). This suggests that the dynamic yield stress of spores could be smaller than that under static pressure.

Given the approximations used in our estimates, and the fact that the tensile stress of the spore exterior layers is probably also temperature sensitive (decreases as the structure melts at high temperatures), our result indicates that spores in ultrafast-heat ($\sim 10^5$ °C/s) and high-temperature processes are more susceptible to increased internal pressures and liable to lose both viability and morphological integrity. It should be noted that such critical heating rates may also be different for other spores, depending upon the degree of dehydration and the permeability of water in the spores.

5. Conclusion

Surface immobilized bacterial spores subjected to sub-second and ultrahigh heating conditions were characterized for spore inactivation and morphological changes. There are two key determinants in spore inactivation. First, maximal peak temperature greater than 700 °C led to 6 logs reduction in spore viability. Second, ultrafast heating of the initial pulse exceeding $\sim 10^5$ °C/s potentiates spore inactivation. Repetitive heating had no discernible effect on spore morphology and survival rate, implying that damage is not cumulative in sub-second heat exposures. At fast heating rates ($\sim 10^4$ °C/s), mutant spores that lack *sspA* *sspB* and *recA* genes were more susceptible to inactivation, indicating that DNA damage contributes to spore inactivation at $\sim 10^4$ °C/s. At higher heating rates of $\sim 10^5$ °C/s, rapid pressurization inside spores is the major contributor to inactivation. The exact correlation between the mechanical changes of spores from morphological studies, and the spore inactivation efficiency remains to be determined. The temperature–time–kill correlation described for spores undergoing a pulse heating process ($\sim 10^3$ °C/s to $\sim 10^5$ °C/s) can be utilized for generating novel strategies to inactivate biological warfare threats due to bacterial spores.

Acknowledgements

This work was funded by a grant from DOD/DTRA (BRBAA08-Per5-H-2-0065). It is greatly thankful to Dr. Peter Setlow from University of Connecticut Health center for kindly providing the wild-type and mutant Bs spores. We also thank Mr. Tim Mangel in the Laboratory for Biological Ultrastructure at the University of Maryland, College Park, for his assistance of shooting SEM images.

Appendix A. Supplementary data

Supplementary data associated with this article can be found, in the online version, at <http://dx.doi.org/10.1016/j.cej.2015.05.021>.

References

- [1] G.W. Gould, History of science – spores Lewis B Perry memorial lecture 2005, *J. Appl. Microbiol.* 101 (2006) 507–513.
- [2] W.L. Nicholson, N. Munakata, G. Horneck, H.J. Melosh, P. Setlow, Resistance of *Bacillus* endospores to extreme terrestrial and extraterrestrial environments, *Microbiol. Mol. Biol. Rev.* 64 (2000) 548–572.
- [3] P. Setlow, Spores of *Bacillus subtilis*: their resistance to and killing by radiation, heat and chemicals, *J. Appl. Microbiol.* 101 (2006) 514–525.
- [4] E. Nadasi, T. Varjas, I. Prantner, V. Virag, I. Ember, Bioterrorism: warfare of the 21st century, *Gene Ther. Mol. Biol.* 11 (2007) 315–320.
- [5] Y. Gilbert, C. Duchaine, Bioaerosols in industrial environments: a review, *Can. J. Civ. Eng.* 36 (2009) 1873–1886.
- [6] V. Kummer, W.R. Thiel, Bioaerosols – sources and control measures, *Int. J. Hyg. Environ. Health* 211 (2008) 299–307.
- [7] T.L. Buhr, A.A. Young, Z.A. Minter, C.M. Wells, D.C. McPherson, C.L. Hooban, C.A. Johnson, E.J. Prokop, J.R. Crigler, Test method development to evaluate hot, humid air decontamination of materials contaminated with *Bacillus anthracis* Δ Sterne and *B. thuringiensis* Al Hakam spores, *J. Appl. Microbiol.* 113 (2012) 1037–1051.
- [8] W.H. Coleman, D. Chen, Y.-Q. Li, A.E. Cowan, P. Setlow, How moist heat kills spores of *Bacillus subtilis*, *J. Bacteriol.* 189 (2007) 8458–8466.
- [9] R. Conesa, P.M. Periago, A. Esnoz, A. Lopez, A. Palop, Prediction of *Bacillus subtilis* spore survival after a combined non-isothermal–isothermal heat treatment, *Eur. Food Res. Technol.* 217 (2003) 319–324.
- [10] O. Couvert, S. Gaillard, N. Savy, P. Mafart, I. Leguerin, Survival curves of heated bacterial spores: effect of environmental factors on Weibull parameters, *Int. J. Food Microbiol.* 101 (2005) 73–81.
- [11] J. Iciek, A. Papiewska, M. Molska, Inactivation of *Bacillus stearothermophilus* spores during thermal processing, *J. Food Eng.* 77 (2006) 406–410.
- [12] J.-H. Mah, D.-H. Kang, J. Tang, Morphological study of heat-sensitive and heat-resistant spores of *Clostridium sporogenes*, using transmission electron microscopy, *J. Food Prot.* 71 (2008) 953–958.
- [13] T.J. Montville, R. Dengrove, T. de Siano, M. Bonnet, W. Schaffner, Thermal resistance of spores from virulent strains of *Bacillus anthracis* and potential surrogates, *J. Food Prot.* 68 (2005) 2362–2366.
- [14] N.E.M. Mustafa, U. Keller, U. Malkus, D. Harmsen, R. Reichelt, A.A. Hussein, S.M. El-Sanousi, Morphological changes induced by wet–heat in *Bacillus cereus* endospores, *Curr. Res. Bacteriol.* 3 (2010) 214–226.
- [15] J.S. Novak, V.K. Juneja, B.A. McClane, An ultrastructural comparison of spores from various strains of *Clostridium perfringens* and correlations with heat resistance parameters, *Int. J. Food Microbiol.* 86 (2003) 239–247.
- [16] F.T. Tabit, E. Buys, The effects of wet heat treatment on the structural and chemical components of *Bacillus sporothermodurans* spores, *Int. J. Food Microbiol.* 140 (2010) 207–213.
- [17] S.D. Gates, A.D. McCartt, P. Lappas, J.B. Jeffries, R.K. Hanson, L.A. Hokama, K.E. Mortelmans, *Bacillus* endospores resistance to gas dynamic heating, *J. Appl. Microbiol.* 109 (2010) 1591–1598.
- [18] S.D. Gates, A.D. McCartt, J.B. Jeffries, R.K. Hanson, L.A. Hokama, K.E. Mortelmans, Extension of *Bacillus* endospore gas dynamic heating studies to multiple species and test conditions, *J. Appl. Microbiol.* 111 (2011) 925–931.
- [19] S.A. Grinshpun, A. Adhikari, C. Li, T. Reponen, M. Yermakov, M. Schoenitz, E. Dreizin, M. Trunov, S. Mohan, Thermal inactivation of airborne viable *Bacillus subtilis* spores by short-term exposure in axially heated air flow, *J. Aerosol Sci.* 41 (2010) 352–363.
- [20] S.A. Grinshpun, C. Li, A. Adhikari, M. Yermakov, T. Reponen, M. Schoenitz, E. Dreizin, V. Hoffmann, M. Trunov, Method for studying survival of airborne viable microorganisms in combustion environments: development and evaluation, *Aerosol Air Qual. Res.* 10 (2010) 414–424.
- [21] S.A. Grinshpun, A. Adhikari, M. Yermakov, T. Reponen, E. Dreizin, M. Schoenitz, V. Hoffmann, S. Zhang, Inactivation of aerosolized *Bacillus atrophaeus* (BG) endospores and MS2 viruses by combustion of reactive materials, *Environ. Sci. Technol.* 46 (2012) 7334–7341.
- [22] E. Johansson, A. Adhikari, T. Reponen, M. Yermakov, S.A. Grinshpun, Association between increased DNA mutational frequency and thermal inactivation of aerosolized *Bacillus* spores exposed to dry heat, *Aerosol Sci. Technol.* 45 (2011) 376–381.
- [23] J.H. Jung, J.E. Lee, S.S. Kim, Thermal effects on bacterial bioaerosols in continuous air flow, *Sci. Total Environ.* 407 (2009) 4723–4730.
- [24] Y.H. Lee, B.U. Lee, Inactivation of airborne *E. coli* and *B. subtilis* bioaerosols utilizing thermal energy, *J. Microbiol. Biotechnol.* 16 (2006) 1684–1689.
- [25] A.D. McCartt, S.D. Gates, J.B. Jeffries, R.K. Hanson, L.M. Joubert, T.L. Buhr, Response of *Bacillus thuringiensis* Al Hakam endospores to gas dynamic heating in a shock tube, *Z. Phys. Chem.* 225 (2011) 1367–1377.
- [26] N. Piekiet, M.R. Zachariah, Decomposition of aminotetrazole based energetic materials under high heating rate conditions, *J. Phys. Chem. A* 116 (2012) 1519–1526.
- [27] K.T. Sullivan, N.W. Piekiet, S. Chowdhury, C. Wu, M.R. Zachariah, C.E. Johnson, Ignition and combustion characteristics of nanoscale Al/AgIO₃: a potential energetic biocidal system, *Combust. Sci. Technol.* 183 (2011) 285–302.
- [28] C. Wu, K. Sullivan, S. Chowdhury, G. Jian, L. Zhou, M.R. Zachariah, Encapsulation of perchlorate salts within metal oxides for application as nanoenergetic oxidizers, *Adv. Funct. Mater.* 22 (2012) 78–85.
- [29] G. Young, N. Piekiet, S. Chowdhury, M.R. Zachariah, Ignition behavior of α -AlH₃, *Combust. Sci. Technol.* 182 (2010) 1341–1359.
- [30] L. Zhou, N. Piekiet, S. Chowdhury, M.R. Zachariah, T-jump/time-of-flight mass spectrometry for time-resolved analysis of energetic materials, *Rapid Commun. Mass Spectrom.* 23 (2009) 194–202.
- [31] L. Zhou, N. Piekiet, S. Chowdhury, M.R. Zachariah, Time-resolved mass spectrometry of the exothermic reaction between nanoaluminum and metal oxides: the role of oxygen release, *J. Phys. Chem. C* 114 (2010) 14269–14275.
- [32] J.M. Mason, P. Setlow, Essential role of small, acid-soluble spore proteins in resistance of *Bacillus subtilis* spores to UV light, *J. Bacteriol.* 167 (1986) 174–178.
- [33] W.L. Nicholson, B. Setlow, P. Setlow, Binding of DNA in vitro by a small, acid-soluble spore protein from *Bacillus subtilis* and the effect of this binding on DNA topology, *J. Bacteriol.* 172 (1990) 6900–6906.
- [34] P. Setlow, I will survive: protecting and repairing spore DNA, *J. Bacteriol.* 174 (1992) 2737–2741.
- [35] B. Setlow, P. Setlow, Small, acid-soluble proteins bound to DNA protect *Bacillus subtilis* spores from killing by dry heat, *Appl. Environ. Microbiol.* 61 (1995) 2787–2790.
- [36] B. Setlow, P. Setlow, Role of DNA repair in *Bacillus subtilis* spore resistance, *J. Bacteriol.* 178 (1996) 3486–3495.
- [37] W.H. Coleman, P. Setlow, Analysis of damage due to moist heat treatment of spores of *Bacillus subtilis*, *J. Appl. Microbiol.* 106 (2009) 1600–1607.
- [38] P. Zhang, L. Kong, P. Setlow, Y.-Q. Li, Characterization of wet–heat inactivation of single spores of *Bacillus* species by dual-trap Raman spectroscopy and elastic light scattering, *Appl. Environ. Microbiol.* 76 (2010) 1796–1805.
- [39] D.L. Popham, J. Helin, C.E. Costello, P. Setlow, Analysis of the peptidoglycan structure of *Bacillus subtilis* endospores, *J. Bacteriol.* 178 (1996) 6451–6458.
- [40] H. Fairhead, B. Setlow, P. Setlow, Prevention of DNA damage in spores and in vitro by small, acid-soluble proteins from *Bacillus* species, *J. Bacteriol.* 175 (1993) 1367–1374.
- [41] B. Setlow, S. Alturi, R. Kitchel, K. Koziol-Dube, P. Setlow, Role of dipicolinic acid in resistance and stability of spores of *Bacillus subtilis* with or without DNA-protective α/β -type small acid-soluble proteins, *J. Bacteriol.* 188 (2006) 3740–3747.

- [42] B. Setlow, E. Melly, P. Setlow, Properties of spores of *Bacillus subtilis* blocked at an intermediate stage in spore germination, *J. Bacteriol.* 183 (2001) 4894–4899.
- [43] S. Nakashio, P. Gerhardt, Protoplast dehydration correlated with heat resistance of bacterial spores, *J. Bacteriol.* 162 (1985) 571–578.
- [44] P. Gerhardt, R.E. Marquis, Spore thermoresistance mechanisms, in: *Regulation of Prokaryotic Development*, American Society for Microbiology, DC, 1986. pp. 43–63.
- [45] S. Kozuka, K. Tochikubo, Permeability of dormant spores of *Bacillus subtilis* to malachite green and crystal violet, *J. Gen. Microbiol.* 137 (1991) 607–613.
- [46] P. Zhang, L. Kong, G. Wang, P. Setlow, Y.Q. Li, Monitoring the wet–heat inactivation dynamics of single spores of *Bacillus* species by using Raman tweezers, differential interference contrast microscopy, and nucleic acid dye fluorescence microscopy, *Appl. Environ. Microbiol.* 77 (2011) 4754–4769.
- [47] E. Melly, A.E. Cowan, P. Setlow, Studies on the mechanism of killing of *Bacillus subtilis* spores by hydrogen peroxide, *J. Appl. Microbiol.* 93 (2002) 316–325.
- [48] S.B. Young, P. Setlow, Mechanisms of killing of *Bacillus subtilis* spores by hypochlorite and chlorine dioxide, *J. Appl. Microbiol.* 95 (2003) 54–67.
- [49] S.B. Young, P. Setlow, Mechanisms of *Bacillus subtilis* spore resistance to and killing by aqueous ozone, *J. Appl. Microbiol.* 96 (2004) 1133–1142.
- [50] B. Setlow, S. Parish, P. Zhang, Y.Q. Li, W.C. Neely, P. Setlow, Mechanism of killing of spores of *Bacillus anthracis* in a high-temperature gas environment, and analysis of DNA damage generated by various decontamination treatments of spores of *Bacillus anthracis*, *Bacillus subtilis* and *Bacillus thuringiensis*, *J. Appl. Microbiol.* 116 (2013) 805–814.
- [51] W. Zhou, S.K. Watt, D.-H. Tsai, V.T. Lee, M.R. Zachariah, Quantitative attachment and detachment of bacterial spores from fine wires through continuous and pulsed DC electrophoretic deposition, *J. Phys. Chem. B* 117 (2013) 1738–1745.
- [52] P.R.N. Childs, *Practical Temperature Measurement*, Butterworth Heinemann, London, UK, 2001.
- [53] J.N. Junior, P.R. de Massaguer, Thermal death kinetics of *B. stearothermophilus* spores in sugarcane must, *J. Food Proc. Eng.* 30 (2007) 625–639.
- [54] B. Setlow, K.A. McGinnis, K. Ragkousi, P. Setlow, Effects of major spore-specific DNA binding proteins on *Bacillus subtilis* sporulation and spore properties, *J. Bacteriol.* 182 (2000) 6906–6912.
- [55] M. Paidhungat, K. Ragkousi, P. Setlow, Genetic requirements for induction of germination of spores of *Bacillus subtilis* by Ca^{2+} -dipicolinate, *J. Bacteriol.* 183 (2001) 4886–4893.
- [56] A. Driks, S. Roels, B. Beall, C.P. Moran Jr., R. Losick, Subcellular localization of proteins involved in the assembly of the spore coat of *Bacillus subtilis*, *Genes Dev.* 8 (1994) 234–244.
- [57] P. Setlow, Small, acid-soluble spore proteins of *Bacillus* species: structure, synthesis, genetics, function, and degradation, *Ann. Rev. Microbiol.* 42 (1988) 319–338.
- [58] R. Kumar, S. Saurav, E.V. Titov, D.A. Levin, R.F. Long, W.C. Neely, P. Setlow, Thermo-structural studies of spores subjected to high temperature gas environments, *Int. J. Heat Mass Transf.* 54 (2011) 755–765.
- [59] Y. Xing, A. Li, D.L. Felker, L.W. Burggraf, Nanoscale structural and mechanical analysis of *Bacillus anthracis* spores inactivated with rapid dry heating, *Appl. Environ. Microbiol.* 80 (2014) 1739–1749.
- [60] M. Peleg, M.B. Cole, Reinterpretation of microbial survival curves, *Crit. Rev. Food Sci. Nutr.* 38 (1998) 353–380.
- [61] A. Driks, *Bacillus subtilis* spore coat, *Microbiol. Mol. Biol. Rev.* 63 (1999) 1–20.
- [62] H. Takamatsu, K. Watabe, Assembly and genetics of spore protective structures, *Cell Mol. Life Sci.* 59 (2002) 434–444.
- [63] S. Ghosh, B. Setlow, P.G. Wahome, A.E. Cowan, M. Plomp, A.J. Malkin, P. Setlow, Characterization of spores of *Bacillus subtilis* that lack most coat layers, *J. Bacteriol.* 190 (2008) 6741–6748.
- [64] T.C. Beaman, P. Gerhardt, Heat resistance of bacterial spores correlated with protoplast dehydration, mineralization, and thermal adaptation, *Appl. Environ. Microbiol.* 52 (1986) 1242–1246.
- [65] S.I. Sandler, *Chemical, Biochemical, and Engineering Thermodynamics*, John Wiley & Sons Inc., Hoboken, NJ, 2006.
- [66] A.G. Li, Y. Xing, L.W. Burggraf, Thermal effects on surface structures and properties of *Bacillus anthracis* spores on nanometer scales, *Langmuir* 29 (2013) 8343–8354.
- [67] E.P. Black, P. Setlow, A.D. Hocking, C.M. Stewart, A.L. Kelly, D.G. Hoover, Response of spores to high-pressure processing, *Compr. Rev. Food Sci. Food Saf.* 6 (2007) 103–119.
- [68] H.-W. Huang, H.-M. Lung, B.B. Yang, C.-Y. Wang, Responses of microorganisms to high hydrostatic pressure processing, *Food Control.* 40 (2014) 250–259.
- [69] Z. Zhang, B. Jiang, X. Liao, J. Yi, X. Hu, Y. Zhang, Inactivation of *Bacillus subtilis* spores by combining high-pressure thermal sterilization and ethanol, *Int. J. Food Microbiol.* 160 (2012) 99–104.